

1 Cryo-EM structure of haemoglobin at 3.2 Å determined with the Volta phase plate

2

3 Maryam Khoshouei¹, Mazdak Radjainia^{2,3}, Wolfgang Baumeister¹ & Radostin Danev^{1*}

4 1 - Department of Molecular Structural Biology, Max Planck Institute of Biochemistry, 82152

5 Martinsried, Germany.

6 2 - The Clive and Vera Ramaciotti Centre for Cryo-EM, Department of Biochemistry and Molecular

7 Biology, Monash University, Victoria, 3800 Melbourne, Australia.

8 3 – Present address: FEI, 5651 GG Eindhoven, The Netherlands.

9 *Correspondence should be addressed to R.D. (danev@biochem.mpg.de).

10 **With the advent of direct electron detectors, the perspectives of cryo-electron microscopy**
11 **(cryo-EM) have changed in a profound way¹. These cameras are superior to previous**
12 **detectors in coping with the intrinsically low contrast of radiation-sensitive organic materials**
13 **embedded in amorphous ice, and so they have enabled the structure determination of several**
14 **macromolecular assemblies to atomic or near-atomic resolution. According to one**
15 **theoretical estimation, a few thousand images should suffice for calculating the structure of**
16 **proteins as small as 17 kDa at 3 Å resolution². In practice, however, we are still far away from**
17 **this theoretical ideal. Thus far, protein complexes that have been successfully reconstructed**
18 **to high-resolution by single particle analysis (SPA) have molecular weights of ~100 kDa or**
19 **larger³. Here, we report the use of Volta phase plate in determining the structure of human**
20 **haemoglobin (64 kDa) at 3.2 Å. Our results demonstrate that this method can be applied to**
21 **complexes that are significantly smaller than those previously studied by conventional**
22 **defocus-based approaches. Cryo-EM is now close to becoming a fast and cost-effective**
23 **alternative to crystallography for high-resolution protein structure determination.**

24 Given the radiation sensitivity of ice-embedded proteins, the low signal-to-noise ratio (SNR) of cryo-
25 EM images is a limitation for SPA⁴, restricting the size range of proteins that can be studied. In 1995,
26 it was estimated, based solely on physical considerations, that the lower molecular weight limit of
27 single particle cryo-EM would be 38 kDa⁵. These considerations presumed the use of a perfect phase

28 plate. It was suggested that the structure of 100 kDa proteins could be determined at 3 Å resolution
29 from only 10,000 particles. Later, it was proposed that the theoretical limit might be even lower if
30 perfect images could be taken^{2, 6}. With the technology at that time and cryo-EM images being far
31 from perfect retaining only 10% of contrast, it seemed that obtaining a 3 Å reconstruction would be
32 reserved for complexes with a molecular weight upwards of 4 MDa⁵. Nowadays, obtaining ~3 Å
33 resolution reconstructions has become almost routine and has been achieved with complexes that
34 are much smaller in size¹. To date, the smallest protein solved to near-atomic resolution by single
35 particle cryo-EM is the 3.8 Å resolution structure of the 93 kDa isocitrate dehydrogenase³. Even so,
36 single particle analysis reconstructions are still strongly biased towards larger symmetric complexes,
37 indicating there is still a long way to go before the full potential of imaging proteins with electrons is
38 reached.

39 The difficulties in routinely obtaining high-resolution reconstructions of small molecular weight
40 proteins are predominantly owed to poor representation of low spatial frequencies in electron
41 micrographs obtained by conventional transmission electron microscopy (CTEM)⁴. CTEM utilises
42 phase contrast produced by spherical aberration (Cs) and the deliberate defocusing of the
43 microscope's objective lens. This approach creates oscillations in the contrast transfer function
44 (CTF) of the microscope with some spatial frequencies of the object being transferred poorly, or not
45 at all. One can compensate for this effect by varying the level of defocus from image to image, which
46 is typically in the range of several hundreds to thousands of nanometres. By combining images that
47 have different levels of contrast for given spatial frequencies an accurate representation of an object
48 can be obtained. Nevertheless, the limitations due to reduced SNR resulting from contrast loss
49 remain.

50 In-focus single particle cryo-EM enabled by the Volta phase plate (VPP) holds the promise of yielding
51 up to a two-fold boost in SNR and therefore enhancing our ability to observe weak phase objects⁷.
52 The SNR of VPP images is high because transfer of contrast of low spatial frequencies is optimal
53 and constant for images taken in focus. Unlike previous phase plate designs, VPP images also retain
54 the high spatial frequencies of the specimen enabling structure determination at near-atomic
55 resolution^{8, 9}. However, in-focus imaging with VPP requires very precise focusing⁸ and the typically

56 strong Cs present in cryo-electron microscopes appears to be a limiting factor in attaining resolutions
57 better than 3 Å by in-focus phase plate-imaging⁸.

58 Enabled by the ability to estimate and correct the phase shift of the VPP in CTFFIND4¹⁰ and
59 RELION2¹¹, we therefore used a hybrid approach combining the strengths of CTEM and VPP¹² (Fig.
60 1). This involves applying a defocus of ~500 nm and correcting for the effects of CTF. We opted to
61 apply this strategy to tetrameric Hgb, which mediates oxygen transport in blood and has a molecular
62 weight of 64 kDa and C2 symmetry. We chose Hgb for its iconic status as the first protein structure
63 alongside myoglobin that was solved using X-ray crystallography by Max Perutz in 1960, coincidentally
64 by overcoming the phase problem of X-ray crystallography¹³.

65 Commercially sourced human Hgb is in the non-functional ferric (Fe³⁺) state referred to as metHgb.
66 After vitrification of the metHgb, the sample was subjected to VPP-enabled imaging with multiframe
67 movies taken at low defocus, as described above. The movies were corrected for motion and
68 radiation damage using MotionCor2¹⁴. Hgb particles were readily discernible in VPP images (Fig.
69 1a) and could be accurately picked because of their high contrast. 2D classification of automatically
70 picked particles resulted in class averages with recognisable features and striking resemblance to
71 the structure of Hgb (Fig. 1c). Class averages were selected for initial model building in EMAN using
72 the common-line technique and taking advantage of the C2 symmetry¹⁵. RELION 3D classification
73 and refinement using half-split datasets of particles yielded the final map¹⁶. The obtained 3D
74 reconstruction had a resolution of 3.2 Å, as determined by the so-called “gold-standard” FSC=0.143
75 criterion.

76 At this level of resolution, side-chain densities and prosthetic haem groups are clearly resolved in
77 our reconstruction (Fig. 2a, Fig. S1). We used an MD-based approach for model building and
78 compared our atomic model with three conformers of ferrous (Fe²⁺) Hgb present in a single crystal
79 (PDB 4N7O) adopting the tight (T) and two relaxed states (R1/R2)¹⁷. Rigid-body fitting was used to
80 dock the α1 subunits yielding a good visual fit with a cross-correlation value of ~69%.
81 Superimposition of docked α1 subunits and corresponding tetramers yields cross-correlation values
82 of 43%, 47% and 62% for T, R1 and R2 states, respectively (Fig. 2b). This observation is in line with

83 the fact that metHgb adopts an R-like state suggesting that conformational states can be determined
84 for small proteins at high-resolution without crystallisation.

85 Our results showcase how cryo-EM can be used to determine which conformational states are
86 present in solution. It has become increasingly clear that simple allosteric models based on discrete
87 states, which are arrested by tight crystal contacts potentially fail to provide a complete
88 structure/function portrait and may be divergent from solution studies¹⁷. Single particle analysis is
89 inherently better suited than crystallography for visualising the full spectrum of conformational states
90 that proteins adopt¹⁸. Obtaining high-resolution structures of solution states may indeed be one of
91 the main applications of structure determination by VPP as a technique complementary to X-ray
92 crystallography and nuclear magnetic resonance spectroscopy.

93 Given the ease of the data acquisition, it can be expected that near-atomic resolution maps will
94 become routine for large parts of the proteome including membrane proteins. In conjunction with
95 improved automation, and next generation direct electron detectors, cryo-EM is likely to become a
96 major player in structure-based small molecule drug discovery for almost any drug target.

97

98 **Methods**

99 **Sample preparation**

100 Human Hgb was commercially sourced (Sigma-Aldrich, St. Louis, MO). Frozen-hydrated specimens
101 were prepared on plasma-cleaned Quantifoil R1.2/1.3 holey carbon EM grids (Quantifoil,
102 Großlöbichau, Germany) using a Vitrobot Mark III (FEI, Hillsboro, OR) 5 s blotting time, 85% humidity
103 and -5 mm blotting offset.

104 **Data acquisition**

105 Automated data collection was performed on a Titan Krios electron microscope (FEI, Hillsboro, OR)
106 operated at 300 kV and equipped with a K2 Summit direct detector, a Quantum energy filter (Gatan,
107 Pleasanton, CA) and an FEI Volta phase plate (FEI, Hillsboro, OR) using SerialEM software. Movies
108 comprising 40 frames and a total dose of 40 e⁻ per Å² were recorded on a K2 Summit direct detection

109 camera (Gatan) at a calibrated magnification of 95,200 corresponding to a magnified pixel size of
110 0.525 Å.

111 **Data processing**

112 The recorded movies were subjected to motion correction with MotionCor2¹⁴. Particles were picked
113 with Gautomatch (developed by Zhang K, MRC Laboratory of Molecular
114 Biology, Cambridge, UK, <http://www.mrc-lmb.cam.ac.uk/kzhang/Gautomatch/>). Subsequently, the
115 283,600 picked particles were extracted in Relion2 using a box size of 100 pixels¹¹. After performing
116 2D classification in Relion2, the best-looking 2D class averages were selected to build an initial
117 model in EMAN using the common-lines approach¹⁵. After two rounds of 3D classification 164,300
118 particles from the best looking class were subjected to 3D auto-refinement in Relion2. The final map
119 was sharpened using a negative B-factor of 200. Local resolution was calculated with *blocres* from
120 the Bsoft package¹⁹. Flexible fitting of the Hgb crystal structure was performed using the NAMD
121 routine in MDFF²⁰ followed by real-space refinement in PHENIX²¹. The data collection, refinement
122 parameters and model statistics are summarised in Table 1.

123

124 **References**

125

- 126 1. Nogales, E. & Scheres, S.H. Cryo-EM: A Unique Tool for the Visualization of
127 Macromolecular Complexity. *Mol Cell* **58**, 677-689 (2015).
- 128 2. Glaeser, R.M. Review: electron crystallography: present excitement, a nod to the past,
129 anticipating the future. *J Struct Biol* **128**, 3-14 (1999).
- 130 3. Merk, A. et al. Breaking Cryo-EM Resolution Barriers to Facilitate Drug Discovery. *Cell* **165**,
131 1698-1707 (2016).
- 132 4. Sigworth, F.J. Principles of cryo-EM single-particle image processing. *Microscopy (Oxf)* **65**,
133 57-67 (2016).
- 134 5. Henderson, R. The potential and limitations of neutrons, electrons and X-rays for atomic
135 resolution microscopy of unstained biological molecules. *Q Rev Biophys* **28**, 171-193 (1995).

- 136 6. Rosenthal, P.B. & Henderson, R. Optimal determination of particle orientation, absolute hand,
137 and contrast loss in single-particle electron cryomicroscopy. *J Mol Biol* **333**, 721-745 (2003).
- 138 7. Danev, R., Buijsse, B., Khoshouei, M., Plitzko, J.M. & Baumeister, W. Volta potential phase
139 plate for in-focus phase contrast transmission electron microscopy. *Proc Natl Acad Sci U S A*
140 **111**, 15635-15640 (2014).
- 141 8. Danev, R. & Baumeister, W. Cryo-EM single particle analysis with the Volta phase plate.
142 *Elife* **5** (2016).
- 143 9. Khoshouei, M. et al. Volta phase plate cryo-EM of the small protein complex Prx3. *Nat*
144 *Commun* **7**, 10534 (2016).
- 145 10. Rohou, A. & Grigorieff, N. CTFFIND4: Fast and accurate defocus estimation from electron
146 micrographs. *bioRxiv* (2015).
- 147 11. Kimanius, D., Forsberg, B.O., Scheres, S. & Lindahl, E. Accelerated cryo-EM structure
148 determination with parallelisation using GPUs in RELION-2. *bioRxiv* (2016).
- 149 12. Danev, R., Tegunov, D. & Baumeister, W. Using the Volta phase plate with defocus for cryo-
150 EM single particle analysis. *bioRxiv* (2016).
- 151 13. Perutz, M.F. et al. Structure of haemoglobin: a three-dimensional Fourier synthesis at 5.5-Å.
152 resolution, obtained by X-ray analysis. *Nature* **185**, 416-422 (1960).
- 153 14. Zheng, S., Palovcak, E., Armache, J.-P., Cheng, Y. & Agard, D. Anisotropic Correction of
154 Beam-induced Motion for Improved Single-particle Electron Cryo-microscopy. *bioRxiv*,
155 061960 (2016).
- 156 15. Tang, G. et al. EMAN2: an extensible image processing suite for electron microscopy. *J Struct*
157 *Biol* **157**, 38-46 (2007).
- 158 16. Scheres, S.H. RELION: implementation of a Bayesian approach to cryo-EM structure
159 determination. *J Struct Biol* **180**, 519-530 (2012).
- 160 17. Shibayama, N., Sugiyama, K., Tame, J.R. & Park, S.Y. Capturing the hemoglobin allosteric
161 transition in a single crystal form. *J Am Chem Soc* **136**, 5097-5105 (2014).

- 162 18. Bai, X.C., Rajendra, E., Yang, G., Shi, Y. & Scheres, S.H. Sampling the conformational space
163 of the catalytic subunit of human gamma-secretase. *Elife* **4** (2015).
- 164 19. Heymann, J.B. & Belnap, D.M. Bsoft: image processing and molecular modeling for electron
165 microscopy. *Journal of structural biology* **157**, 3-18 (2007).
- 166 20. Chan, K.Y., Trabuco, L.G., Schreiner, E. & Schulten, K. Cryo-electron microscopy modeling
167 by the molecular dynamics flexible fitting method. *Biopolymers* **97**, 678-686 (2012).
- 168 21. Adams, P.D. et al. PHENIX: a comprehensive Python-based system for macromolecular
169 structure solution. *Acta Crystallogr D Biol Crystallogr* **66**, 213-221 (2010).

170

171 **Accession codes**

172 The cryo-EM map and atomic coordinates of Hgb were deposited to the Electron Microscopy Data
173 Bank (EMDB) and Protein Data Bank (PDB) under accession codes EMD-3488 and PDB-5ME2,
174 respectively. Raw data was made available at the Electron Microscopy Pilot Image Archive
175 (EMPIAR) with accession code EMPIAR-10105.

176 **Acknowledgments**

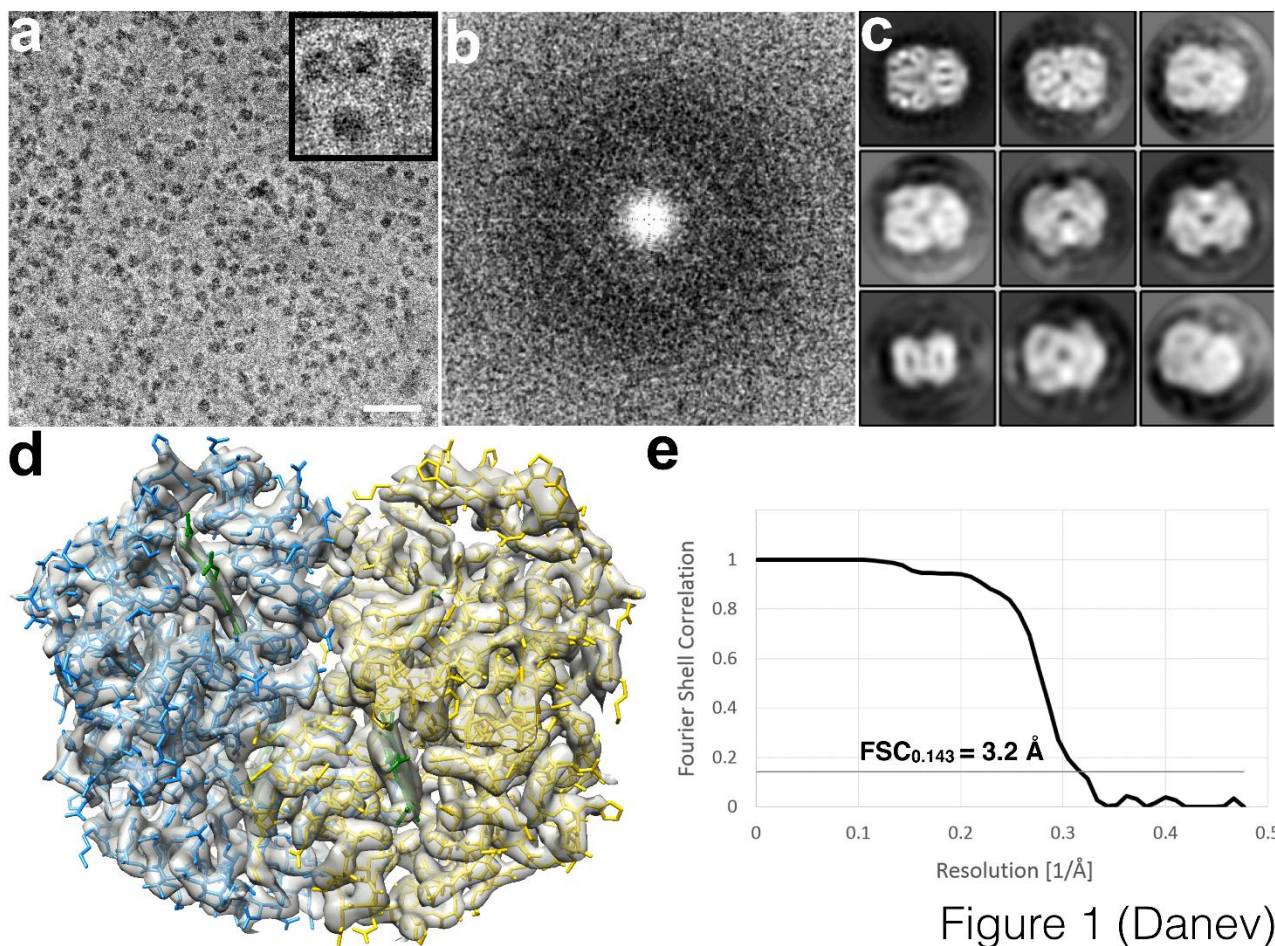
177 We thank Prof. Jürgen Plitzko for his technical support. We also acknowledge Dr. Alexis Rohou
178 and Sjors Scheres for support with CTFFIND4 and Relion2, respectively. We thank Dr. Matthew
179 Belousoff for model building of the Hgb atomic model. We also thank Dr. Mike Strauss and Dr.
180 Shelley Robison for critical reading of the manuscript. This work was supported by the Multi-modal
181 Australian ScienceS Imaging and Visualisation Environment (www.massive.org.au).

182 **Author contributions**

183 MK, MR and RD were responsible for the conception, design, data analysis and interpretation of
184 experiments. MK performed sample preparation and imaging. All authors wrote the manuscript.

185 **Competing financial interests**

186 RD is a co-inventor in US patent US9129774 B2 "Method of using a phase plate in a transmission
187 electron microscope". WB is on the Scientific Advisory Board and MR an employee of FEI Company.



188

189 **Figure 1.** Phase plate-imaging of 64 kDa Hgb. (a) Electron micrograph of methHgb recorded at ~500
190 nm underfocus with the Volta phase plate (VPP) (scale bar = 30nm). (b) Power spectrum of the
191 image in (a), featuring contrast transfer function (CTF) Thon rings permitting defocus and phase shift
192 estimation. (c) 2D class averages of Hgb showing secondary structure elements in projection. (d)
193 Reconstructed 3D map and model of Hgb. (e) (Gold Standard?) Fourier shell correlation (FSC) plot
194 indicating a resolution of 3.2 Å according to the FSC=0.143 criterion.

195

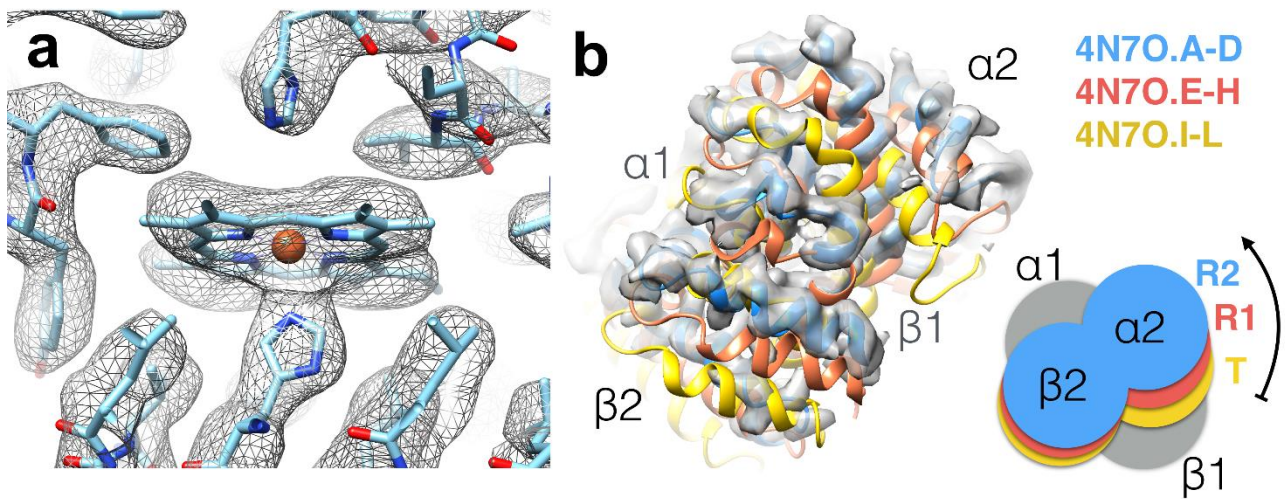


Figure 2 (Danev)

196

197 **Figure 2.** Hgb at 3.2 Å resolution. (a) The iron atom of the prosthetic haem group is coordinated by
198 the proximal histidine residue, as evidenced by a strong density connecting them. (b) VPP
199 reconstruction fitted with 3 conformers of Hgb present in crystal structure PDB 4N7O. The
200 reconstructed 3D map agrees best with chains A-D of PDB 4N7O representing the R2 state of Hgb.

201

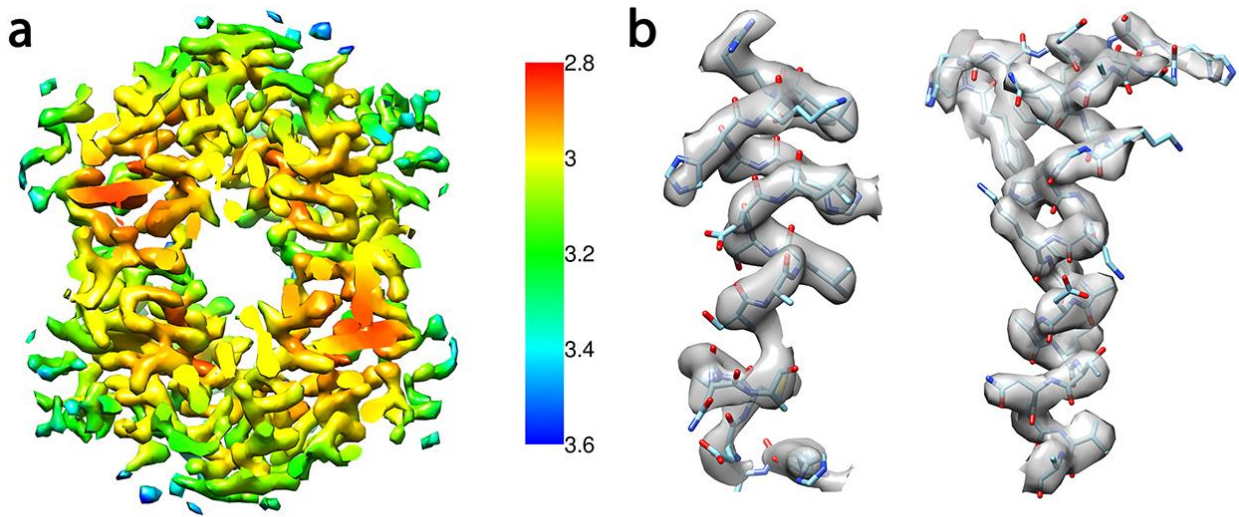


Figure-S1 (Danev)

202

203 **Figure S1.** (a) Local resolution estimation. (b) Magnified details of the 3D map with refined model.

204

Table 1

Data Collection

Particles used in final 3D refinement	175,374
Pixel size (Å)	0.525
Defocus (µm)	-0.5
Voltage (kV)	300
Electron dose (e ⁻ Å ⁻²)	40

Rms deviations

Bonds (Å)	0.009
Angles (°)	0.808

Validation

Clashcore, all atoms	4.5
Good outliers (%)	0.0

Ramachandran plot

Favored (%)	97.13
Allowed (%)	2.87
Outliers (%)	0.0

Refinement

Resolution (Å)	3.2
Map sharpening B-factor (Å ²)	-200
Fourier Shell Correlation	0.143